

## Coherence Resonance Near a Hopf Bifurcation

O. V. Ushakov,<sup>1,\*</sup> H.-J. Wünsche,<sup>1</sup> F. Henneberger,<sup>1</sup> I. A. Khovanov,<sup>1,2</sup> L. Schimansky-Geier,<sup>1</sup> and M. A. Zaks<sup>1</sup>

<sup>1</sup>*Institut für Physik, Humboldt Universität zu Berlin, Newtonstrasse 15 12489 Berlin, Germany*

<sup>2</sup>*Department of Physics, Saratov State University, 410026 Saratov, Russia*

(Received 8 February 2005; published 14 September 2005)

We report on the observation of coherence resonance for a semiconductor laser with short optical feedback close to Hopf bifurcations. Noise-induced self-pulsations are documented by distinct Lorentzian-like features in the power spectrum. The character of coherence is critically related to the type of the bifurcation. In the supercritical case, spectral width and height of the peak are monotonic functions of the noise level. In contrast, for the subcritical bifurcation, the width exhibits a minimum, translating into resonance behavior of the correlation time in the pulsation transients. A theoretical analysis based on the generic model of a self-sustained oscillator demonstrates that these observations are of general nature and are related to the fact that the damping depends qualitatively different on the noise intensity for the subcritical and supercritical case.

DOI: [10.1103/PhysRevLett.95.123903](https://doi.org/10.1103/PhysRevLett.95.123903)

PACS numbers: 42.65.Sf, 05.40.-a, 42.55.Px

The influence of noise on oscillatory motion is a subject of permanent interest, both for fundamental and practical reasons [1–3]. Noise-induced dynamics governs many physical, chemical, and biological processes, reaching from climatic changes [4] to the mammalian cochlea [5,6]. A phenomenon of particular importance in this context is coherence resonance (CR) [7–9]. Here, noise plays a constructive role: It induces regular oscillations of the state variables with a maximum degree of coherence at a certain, finite noise level [10].

CR results from the interplay between noise and nonlinearity. Well established, both by theory and experiment, is the CR in excitable systems [8,9]. Here, quasiregular spiking sequences originate from the existence of a threshold in conjunction with a refractory period, during which the system does not respond to external perturbations. In this Letter, we focus on CR in nonexcitable systems. Noisy precursors of period doubling as well as torus bifurcations have been numerically investigated in Ref. [11]. Resonance-like behavior close to the onset of a supercritical Hopf bifurcation has been found in computer simulations [12,13] and observed experimentally for plasma waves [14,15] and electro-chemical reactions [16]. However, in all these studies, the question how the type of the bifurcation controls the noise dynamics and, in particular, whether this manifests in the existence of CR has not been explicitly addressed.

In what follows, we examine systematically the prototype case of a Hopf bifurcation. We demonstrate that noise-induced resonances occur for both the subcritical and supercritical type. However, the specific response is crucially determined by the character of the bifurcation. The experimental system can be adjusted close to both types of bifurcations, allowing us to investigate the influence of noise under otherwise identical physical conditions. Analytical and numerical results are obtained from studies of canonical models for each type of bifurcation, yielding

full qualitative agreement with the experimental data and demonstrating hence the universal character of our observations.

The experimental system under investigation is a semiconductor laser subjected to delayed optical feedback. Use of a multisection waveguide configuration allows us to implement the ultra-short-cavity regime, where the delay is much shorter than the period of the relaxation oscillations of the solitary laser. In addition, multisection lasers enable us to tune the feedback parameters in a wide range and, thus, to explore the phase space of the device in a systematic way. The laser structure (see Fig. 1) of the

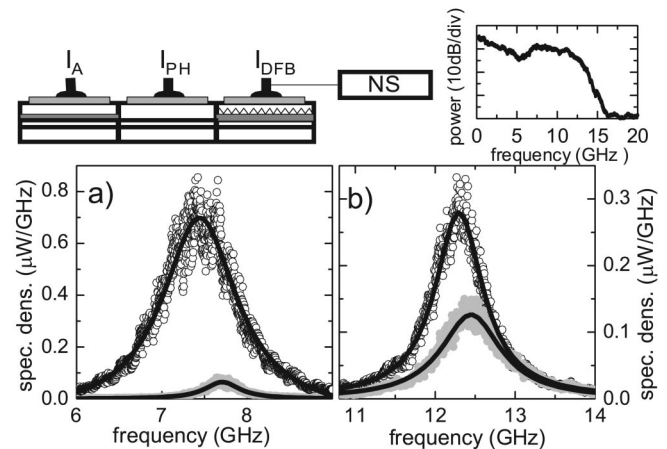


FIG. 1. Upper left panel: Scheme of the multisection laser device; see text for explanations. Upper right panel: Power spectrum of electrical noise. Lower panel: Power spectra of the device under the influence of noise. (a) Before the supercritical Hopf bifurcation without external noise (lower plot) and at optimum noise level (upper plot), solid lines are fits with a Lorentzian shape ( $I_{\text{DFB}} = 70$  mA,  $I_{\text{PH}} = 11.8$  mA,  $I_{\text{A}} = 5.62$  mA). (b) The same for the subcritical case ( $I_{\text{DFB}} = 70$  mA,  $I_{\text{PH}} = 98.2$  mA,  $I_{\text{A}} = 30.6$  mA).

present study consists of a single-mode  $1.55 \mu\text{m}$  distributed feedback laser, a phase section of higher band-gap material, and a  $1.55 \mu\text{m}$  amplifier section (no Bragg grating), all with the same length dimension of a few  $100 \mu\text{m}$ . While the current  $I_{\text{DFB}}$  pumps the laser above threshold, the extra injections  $I_{\text{PH}}$  and  $I_{\text{A}}$  serve to adjust phase and strength of the feedback as appropriate [17]. When changing these control currents, the device undergoes a variety of generic bifurcations [17,18], among them the subcritical and the supercritical Hopf bifurcations being of interest here. In both cases, the laser emission switches from steady-state to a self-pulsation mode; however, the limit cycle appears either in a local way with infinitely small amplitude or nonlocally by a finite amplitude step.

Details of the experimental setup can be found elsewhere [17,18]. Power spectra of the device emission are recorded by a spectrum analyzer (R&S FSP 9) of 40 GHz bandwidth. Electrical broadband noise is generated by a  $50 \Omega$  resistor at room temperature and then amplified by three electrical amplifiers (SHF100CP) with 25 GHz bandwidth. The power spectrum of the noise (Fig. 1) is practically white in the relevant frequency range. The noise is added to the laser injection current  $I_{\text{DFB}}$  (“NS” in Fig. 1) and thus imprinted in the carrier density. In order to avoid a shift of the operation point, the dc component is filtered by a broadband bias tee (SHFBT45) with a bandwidth of 45 GHz. While the average of the noise signal itself is zero, the noise intensity is Gaussian distributed with a mean-value adjusted experimentally by a tunable attenuator (HP8494B/11 dB) with an accuracy of 1 dB. The maximally accessible value is  $D = -20 \text{ dBm/GHz}$ .

The device is capable of two stable self-pulsations with distinctly different frequencies determined by their specific physical origin [18]. The beating of two longitudinal compound-cavity modes gives rise to pulsations with frequencies  $f > 20 \text{ GHz}$ . Here, we focus on the low-frequency pulsations ( $f \leq 12 \text{ GHz}$ ) arising from undamped relaxation oscillations due to dispersive  $Q$  switching. In order to elucidate the influence of noise, the injection currents are adjusted close to the respective bifurcation point, where the steady-state emission is still stable. Even in the absence of external noise, as documented by the weak features in the power spectra of Fig. 1, precursors of the pulsations are observed for both types of bifurcations. Those precursors are induced by the intrinsic noise of the device. When adding external noise, the precursors develop into pronounced resonance features. The frequencies of the peaks are different, as the gain-index coupling is different in the two operation points. When moving the device away from the bifurcations by changing the currents, the resonance effect disappears gradually. Eventually, the noise creates merely fluctuations in the laser emission, as indicated by an increased noise floor in the power spectrum. To analyze the spectral response quantitatively, the data are fitted by a Lorentzian

line-shape function with peak frequency  $\omega_p$ , a full width at half maximum  $2\Delta_\omega$ , and peak height  $H$ . The width  $\Delta_\omega$  translates by Fourier transformation in a correlation time  $\tau_c \sim 1/\Delta_\omega$ . There is only very little shift of the peak frequency so that the quality factor  $Q = \omega_p/\Delta_\omega$  is an inverse function of the width. A measure characterizing the noise-induced response is the signal-to-noise ratio [7,9,11]

$$\beta = HQ = H\omega_p/\Delta_\omega. \quad (1)$$

As seen in the Fig. 2, again in both cases,  $\beta$  is a non-monotonic function of the noise intensity, demonstrating the existence of an optimum noise level. However, qualitative differences between the bifurcations turn out, when height and width are considered. In the supercritical case,  $H$  and  $\Delta_\omega$  increase monotonically, although with different slopes. In particular, the height saturates at higher noise intensities, as the system nonlinearities limit the oscillation amplitude. In contrast, the width exhibits a clear minimum at a certain noise intensity for the subcritical bifurcation. In the time domain, this means a maximum of  $\tau_c$ , similarly to the CR of excitable systems [8]. However, there is a marked difference: The noise-induced peak is already present at infinitely small noise intensities in the present case, whereas the threshold of excitable systems produces an abrupt occurrence at a certain noise level. The relaxation-oscillation self-pulsations are also born in a supercritical torus bifurcation when the higher-frequency mode-beating pulsations are already present. Locating the system on the stable limit cycle and adding noise, the result is qualitatively the same as in Figs. 2(a) and 2(c) for the case of a stable focus. This suggests that, irrespective of the specific oscillator involved, the type of the noise resonance is determined by the subcritical or supercritical character of the bifurcation. The succeeding analysis demonstrates that the above observations are indeed of much wider

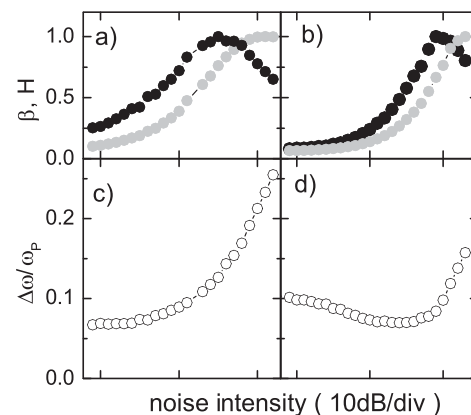


FIG. 2. Peak height (gray dots), normalized width (open dots), and signal-to-noise ratio (black dots) versus noise intensity as deduced from the power spectra by Lorentzian fits. Note the log scale. (a),(c) Supercritical bifurcation, (b), (d) Subcritical bifurcation. Maxima of curves are normalized to unity.

reach, as they uncover generic scenarios close to a Hopf bifurcation.

An elementary model that adequately reproduces the above findings is given by the Langevin equation

$$\dot{z} = -i\omega_0 z + zF(z) + \sqrt{2D}\xi(t) \quad (2)$$

used in many different contexts, e.g., to describe a self-sustained oscillator in rotating wave approximation [19]. Here  $z = x + iy$  is a complex amplitude,  $\omega_0$  is the eigenfrequency, and  $\xi(t) = \xi_x(t) + i\xi_y(t)$  represents a complex white noise source with two independent components.  $F(z)$  is a nonlinear function that defines the type of the bifurcation [20]. For the supercritical Hopf bifurcation, it has the form  $F(z) = F_1(r) = a_1 - r^2$  with  $r = |z| = \sqrt{x^2 + y^2}$ . Periodic motion arises at  $a_1 = 0$ . Alternatively, the subcritical Hopf bifurcation is described by  $F(z) = F_2(r) = a_2 + r^2 - r^4$ . Here, the limit cycle is generated by a saddle-node bifurcation at  $a_2 = -1/4$ , while the Hopf bifurcation takes place at  $a_2 = 0$ . Below, we set  $\omega_0 = 1$  and use the values  $a_1 = -0.01$  and  $a_2 = -0.3$ . In the absence of noise, this choice adjusts the system before the cycle birth,  $z = 0$  being a stable fixed point and  $dr/dt < 0$  everywhere outside this point. We emphasize that excitability (see, e.g., [21]) is excluded under such conditions, as the amplitude of any perturbation will monotonically decay. Therefore, the physics behind the response to noise is qualitatively different. Note that a reduced phase description is insufficient in the present case and the full amplitude dynamics has to be treated.

Though of general nature, the model (2) accounts for the essential features of the laser dynamics. In the latter, the character of the bifurcation changes from subcritical to supercritical at a degeneracy point, where the branching coefficient vanishes [17]. In the first operation point [Fig. 1(a)], a stable focus transforms into a limit cycle, whereas, in the second case [Fig. 1(b)], the laser is close to a saddle-node bifurcation of periodic states, after which a stable fixed point coexists with a limit cycle.

Results of numerical simulation of (2) are summarized in Fig. 3. For a comparison with the experimental findings, the computed power spectra are also fitted by a Lorentzian line-shape function. Indeed, resonance-type response is found for both bifurcations and, even more strikingly, width and peak height exhibit the same qualitative behavior for the subcritical and supercritical type as seen in the experiment.

More insight in the noise-induced motion is obtained by the subsequent analytical treatment. Introduction of the variable  $w = u + iv = z \exp(i\omega_0 t)$  yields

$$\dot{w} = wF(w) + \sqrt{2D}\xi_w(t), \quad (3)$$

where the noise  $\xi_w(t)$  has the same properties as  $\xi(t)$ . The spectrum  $S$  of the variable  $x$  (or  $y$ ) at  $\omega > 0$  is related to the spectrum of the variable  $u$  (or  $v$ ) by  $S_x(\omega) = S_u(\omega + \omega_0)/2$ . Motivated by the experimental and numerical

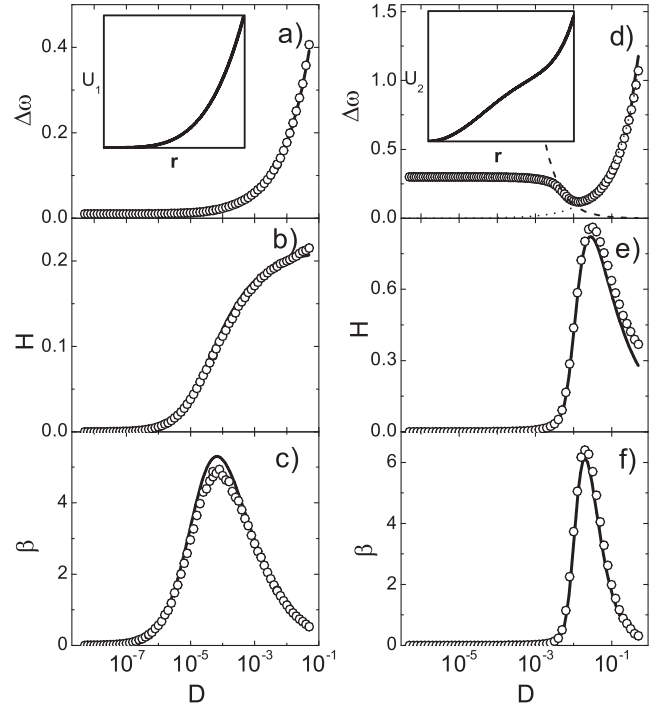


FIG. 3. Width ( $\Delta_\omega$ ), peak height ( $H$ ), and signal-to-noise ratio ( $\beta$ ) versus noise intensity ( $D$ ) as obtained from the theoretical analysis. Left column (a)–(c) Supercritical bifurcation ( $F = F_1$ ). Right column (d)–(f) Subcritical bifurcation ( $F = F_2$ ). Symbols “O” represent the numerical solution of (2), lines are obtained from the analytical treatment. Insets: Shape of the potentials  $U_1(r)$  and  $U_2(r)$ . Dashed lines in (d) show the asymptotic behavior  $D^{-1}$  and  $D^{2/3}$ , respectively (see text for details).

data, we use the Lorentzian ansatz

$$S_u(\omega) = \frac{2D}{\pi(\Delta_\omega^2 + \omega^2)}. \quad (4)$$

For  $F = F_1$ , the application of (4) has been justified in Refs. [3,19]. Then, width and peak height are interrelated by  $H = 2D/(\pi\Delta_\omega^2)$ .  $\Delta_\omega$  is determined by the Parseval theorem, which provides in combination with a Lorentzian spectrum  $\int_{-\infty}^{\infty} S_u(\omega)d\omega = 2D/\Delta_\omega = \langle u^2 \rangle = \langle r^2 \rangle/2$  and thus

$$\Delta_\omega = 2D/\langle r^2 \rangle, \quad (5)$$

$$\langle r^2 \rangle = \int_0^\infty r^2 P(r) dr. \quad (6)$$

The amplitude  $r$  has a Rayleigh-like distribution [3,19]

$$P(r) = Nr \exp(-U(r)/D), \quad (7)$$

where  $N$  is a normalization constant. The potential  $U(r) = -\int rF(r)dr$  is given by  $U_1(r) = -a_1 r^2/2 + r^4/4$  for the supercritical bifurcation and by  $U_2(r) = -a_2 r^2/2 - r^4/4 + r^6/6$  for the subcritical case. For  $U_1(r)$ , the integral (6) can be written explicitly in terms of exponential and

error functions. In the parameter range of interest, a sufficiently accurate approximation for the spectral width is

$$\Delta_{\omega}^{(1)} = -\frac{a_1}{2} + \frac{\sqrt{a_1^2 + 12D}}{2}. \quad (8)$$

It is seen that the  $\Delta_{\omega}^{(1)}$  stays practically constant for small noise and increases as  $\sqrt{D}$  at larger  $D$  [Fig. 3(a)]. Instead, the peak height grows initially like  $H \sim D$  and saturates for stronger noise [Fig. 3(b)].

In the subcritical case, the integral (6) is evaluated numerically. The range of the function  $U_2(r)$  relevant in the integration is set by the noise level, since the maximum of the distribution (7) shifts to larger  $r$  with increasing  $D$ . For small noise levels, the term  $\sim r^2$  dominates and, consequently,  $\Delta_{\omega}^{(2)}$  is constant as in the supercritical case. For moderate noise, the second term becomes important and the potential is almost a linear function  $U_2 \sim r$  (inset, Fig. 3) so that  $\Delta_{\omega}^{(2)} \sim D^{-1}$  decreases with increasing noise. Eventually, the third term in  $U_2$  takes over, producing again an increase  $\Delta_{\omega}^{(2)} \sim D^{2/3}$ . In this way, the spectral width becomes a nonmonotonic function with a distinct minimum at a certain noise level. We note that this behavior is not restricted to the particular form of  $F_2$  used above. It originates from the competition between the destabilizing term  $\sim r^2$  and a higher-order stabilizing term, being generic for subcritical bifurcations. The model predicts in addition a maximum of the peak height  $H$  [Fig. 3(e)]. Such maximum has not been observed in the experiment, probably due to specific amplitude nonlinearities in the laser, not accounted for in the model.

In conclusion, we have demonstrated that resonance phenomena driven by noise are a general concomitant to a Hopf bifurcation. However, while the existence of an optimum noise level is a common feature for both types of bifurcations, the physics behind the resonance effect is qualitatively different. In the supercritical case, the increase of the signal-to-noise ratio is produced by the spectral peak height, that is, by an increase of the oscillation amplitude. The width is initially only slightly affected, but increases steeply for stronger noise, weakening the coherence. Resonance-like behavior originates from the competition between the growth of height and width. In contrast, for the subcritical type, the spectral width itself exhibits a minimum. Here, the noise improves, indeed, the quality factor as well as the temporal coherence of the oscillation transients. In a strict sense, only this kind of response represents truly CR. These qualitative differences between the subcritical and supercritical case are related to amplitude dynamics, whereas the effect of noise on the frequencies is insignificant. The degree of coherence depends on the effective damping, determined by the local steepness of  $U(r)$  at the maximum of the amplitude distribution. Growth of the noise shifts this maximum towards larger  $r$ . In the

supercritical case, the damping is a monotonic function of the amplitude and, hence, of the noise. The subcritical case is distinguished by a nonmonotonic relation between the local slope of the potential and the noise intensity. Accordingly, in a certain intermediate range of noise, weakly damped coherent oscillations with moderate amplitudes are excited.

Our experimental study for semiconductor laser implies various applications in the area of optical data communication. It will be interesting to study also biological systems in this regard and even ensembles of CR systems.

This work was supported by Deutsche Forschungsgemeinschaft within the Sfb 555. I. A. Kh. wishes to thank the AvH-Stiftung for support.

---

\*Electronic address: ushakov@physik.hu-berlin.de

- [1] H. Haken, *Rev. Mod. Phys.* **47**, 67 (1975).
- [2] R. Graham, *J. Stat. Phys.* **54**, 1207 (1989).
- [3] H. Risken, *Fokker-Planck Equation* (Springer, Berlin, 1984).
- [4] A. Ganopolski and S. Rahmstorf, *Phys. Rev. Lett.* **88**, 038501 (2002).
- [5] T. Risler, J. Prost, and F. Jülicher, *Phys. Rev. Lett.* **93**, 175702 (2004).
- [6] R. Stoop and A. Kern, *Phys. Rev. Lett.* **93**, 268103 (2004).
- [7] Hu Gang *et al.*, *Phys. Rev. Lett.* **71**, 807 (1993).
- [8] A. Pikovsky and J. Kurths, *Phys. Rev. Lett.* **78**, 775 (1997).
- [9] B. Lindner, J. Garcia-Ojalvo, A. Neiman, and L. Schimansky-Geier, *Phys. Rep.* **392**, 321 (2004).
- [10] CR is distinguished from stochastic resonance by the fact that, for the latter, a stochastic process synchronizes to a regular external signal at an optimum noise level.
- [11] A. Neiman, P.I. Sparin, and L. Stone, *Phys. Rev. E* **56**, 270 (1997).
- [12] Z. Hou and H. Xin, *Phys. Rev. E* **60**, 6329 (1999); A. F. Rozenfeld, C. J. Tessone, E. Albano, and H. S. Wio, *Phys. Lett. A* **280**, 45 (2001); G. S. Jeon and M. Y. Choi, *Phys. Rev. B* **66**, 064514 (2002); S. Katsev and I. L. Heureux, *Phys. Rev. E* **61**, 4972 (2000).
- [13] W. Ebeling, H. Herzog, W. Richert, and L. Schimansky-Geier, *Z. Angew. Math. Mech.* **66**, 141 (1986).
- [14] L. I and J. Liu, *Phys. Rev. Lett.* **74**, 3161 (1995).
- [15] A. Dinklage, C. Wilke, and T. Klinger, *Phys. Plasmas* **6**, 2968 (1999).
- [16] I. Z. Kiss *et al.*, *Phys. Rev. E* **67**, 035201(R) (2003).
- [17] S. Bauer, O. Brox, J. Kreissl, and B. Sartorius, *Phys. Rev. E* **69**, 016206 (2004).
- [18] O. Ushakov, S. Bauer, O. Brox, H.-J. Wünsche, and F. Henneberger, *Phys. Rev. Lett.* **92**, 043902 (2004).
- [19] R. D. Hempstead and M. Lax, *Phys. Rev.* **161**, 350 (1967).
- [20] V. I. Arnold, *Geometrical Methods in the Theory of Ordinary Differential Equations* (Springer, New York, 1982).
- [21] E. M. Izhikevich, *Int. J. Bifurcation Chaos Appl. Sci. Eng.* **10**, 1171 (2000).